J. Fluid Mech. (2004), *vol.* 521, *pp.* 217–239.
DOI: 10.1017/S0022112004001788 Printed in the United Kingdom

Inner scaling for wall-bounded flows subject to large pressure gradients

By T. B. NICKELS

Department of Engineering, Cambridge University, Trumpington Street, Cambridge CB2 1PZ, UK

(Received 31 July 2003 and in revised form 10 August 2004)

In this paper the scaling of the mean velocity profile and Reynolds stresses is considered for the case of turbulent near-wall flows subjected to strong pressure gradients. Strong pressure gradients are defined as those in which the streamwise pressure gradient non-dimensionalized with inner variables, p_x^+, is greater than 0.005. A range of values of this parameter ($-0.02 < p_x^+ < 0.06$) is examined in this paper. An appropriate functional form for the mean velocity profile is developed and used to parameterize available data. A physical model for the parametric variation with pressure gradient is then developed. This model is based on the concept of a universal critical Reynolds number for the sublayer which explains (both qualitatively and quantitatively) the variation of the important parameters in the inner flow. In particular this gives an explanation for the shift in the apparent log-law due to pressure-gradient effects and provides an appropriate scaling for the Reynolds stresses. It is shown that this model is not only physically plausible but is also consistent with the available data.

1. Introduction

The law of the wall and the related logarithmic overlap law have formed the basis of analysing turbulent boundary layers for some time. Despite some recent controversy over their applicability and basis (George & Castillo 1997; Buschman & Gad-el-Hak 2003), they still provide useful tools for parameterizing turbulent boundary layer velocity profiles. The logarithmic law is derived as the asymptotic form of the boundary layer mean velocity profile at very high Reynolds number (strictly applicable in the limit of infinite Reynolds number). Despite this restriction, it is frequently applied as a means for parameterizing data, and even for evaluating wall shear stress (using the 'Clauser chart' method), in situations where this condition is not met. In particular it is often used where the Reynolds number of the boundary layer is too small for an overlap region to exist. Another situation in which the logarithmic law is known to 'break down' is in the case of strong streamwise pressure gradients. This breakdown appears as a shift in the profile above or below the traditional log-law and may also be associated with a change in shape of the profile (Nagano, Tagawa & Tsuji 1991; Spalart & Watmuff 1993; Fernholz & Warnack 1998). As a result, various researchers have investigated this effect with the objective of specifying conditions under which the logarithmic law may be expected to apply (Huffman & Bradshaw 1972; Spalart 1986; Österlund *et al.* 2000). These often take the form of a critical value of Reynolds number or pressure-gradient parameter beyond which there is a significant departure from universal behaviour. Whilst this information is

useful, it would seem that any departure from universal behaviour would be gradual rather than occurring at, or around, a certain parameter value.

The author's interest in this area arose whilst trying to parameterize low-Reynolds-number boundary layer profiles, some involving strong pressure gradients. It was found that the usual tools (law of the wall, law of the wake etc.) had serious problems in dealing with these flows. This is not surprising since they are based on assumptions not valid for these conditions. In their usual forms they also have certain problems with satisfying the correct boundary conditions and asymptotic behaviour.

In order to proceed further, it was necessary to construct a function that would be suitable for use in these low-Reynolds-number, strong-pressure-gradient flows. The idea was to use known boundary conditions and asymptotic forms to construct a functional form that behaved sensibly under all conditions of interest, whilst retaining the desirable essentials of the usual approach. This tool could then be used to examine the changes in the flow under the influence of strong pressure gradients.

When this was done it was found, as already noted, that one of the parameters (which corresponds closely with the log-law intercept) does indeed vary with the applied pressure gradient (this is the 'shift' mentioned above). This led to the development of a simple model, which explains how and why the parameter varies. After studying much data, it appeared that the model and the new functional form provided a very useful description of boundary layers at low Reynolds number and in strong pressure gradients, and hence the results of this development and investigation may be of interest to other researchers in the field.

The paper may be loosely divided into two parts. The first part develops the new empirically based functional form for the mean velocity profile which correctly takes into account the appropriate boundary conditions and asymptotic behaviour, whilst retaining the basic overall features of the classical approach (such as the logarithmic asymptotic form, the linear sublayer and the wall-wake structure). This form is developed merely as a tool to analyse the existing data in a consistent and objective manner so as to identify important changes in parameters with the pressure gradient.

The second part develops the critical sublayer Reynolds number model which simply explains (both qualitatively and quantitatively) the way in which the traditional law of the wall is modified by pressure gradients. This part is considered to be the major contribution of the research.

2. The functional form for the mean velocity profile

In this section a useful functional form for the mean velocity profile for wall-bounded flows is developed. When analysing data for small parametric effects it is important to have a sensible functional form to fit to the data which has the correct asymptotic and boundary conditions. This is particularly important when examining low-Reynolds-number flows with pressure gradients, where traditional formulations are not ideal since they assume a function based on the high-Reynolds-number asymptotic form of the equations. The approach adopted here is unashamedly constructive, i.e. plausible functions with the correct boundary conditions and asymptotic forms are constructed where necessary (when they cannot be deduced otherwise). The form found is simply a useful tool for the parameterization of the data.

As already discussed, the traditional form for the variation of the streamwise component of the mean velocity, U, with the distance normal to the wall, y, is composed of two parts: an inner part and an outer part. In the inner region close to

the wall it is traditionally assumed that the only important parameters are the wall shear stress, τ_w, the kinematic viscosity, ν and the fluid density, ρ. This leads to

$$U^+ = f(y^+), \tag{2.1}$$

where $U^+ = U/U_\tau$, $y^+ = yU_\tau/\nu$, $U_\tau = \sqrt{\tau_w/\rho}$ is the wall-shear velocity and $f(y^+)$ is some function of y^+ only.

In the outer part of the flow it is usual to assume a defect law of the form

$$\frac{U_1 - U}{U_\tau} = g(\eta), \tag{2.2}$$

where U_1 is the free-stream velocity far from the wall, i.e. $U(y)$ in the limit $y \to \infty$ and $\eta = y/\delta$ in the case of boundary layers (δ is a measure of the boundary layer thickness which might, for example, be taken as the value of y where $U(y) = 0.99U_1$ – the 99% thickness). In the case of fully developed pipe or channel flow U_1 would be the centre-line velocity and $\eta = y/R$ for pipe flow (R is the pipe radius) or $\eta = y/h$ for channel flow (h is the distance from the centreline to the wall). Once these forms are assumed, overlap arguments (Millikan 1938) suggest that, in the limit of infinite Reynolds number, there will be a region ($y^+ \to \infty$ and $\eta \to 0$) in which the mean velocity profile has the form

$$U^+ = \frac{1}{\kappa}\ln(y^+) + C, \tag{2.3}$$

where κ and C are universal constants. It must be emphasized that this only applies in some region that is not too close to the wall and is also far from the outer edge of the layer. It only strictly applies as $\delta^+ = \delta U_\tau/\nu \to \infty$ ($\delta^+ = y^+/\eta$). Coles (1956) extended this form to take account of the outer part of the flow by adding a wake function, leading to

$$U^+ = \frac{1}{\kappa}\ln(y^+) + C + w(\eta), \tag{2.4}$$

where $w(\eta)$ is the required wake function. This gives a reasonable fit to experimental data away from the wall. There have been various suggestions for extending this form to cover the region near the wall as well, the most commonly used being due to Van Driest (1956) and Reichardt (1951). Both these forms (and many others) are functions which attempt to give the correct Taylor series expansion near the wall based on the appropriate boundary conditions and asymptote to a logarithmic form (as given by (2.3)) far from the wall. These may then be combined with a wake function in an attempt to fit the whole mean velocity profile from the wall to the edge of the layer.

Whilst these functional forms (alone and in various combinations) are satisfactory in many situations, there are anomalous features which make them unsatisfactory for the present analysis. These problems will be discussed during the development of the new form.

The form derived here has a simple three-layer structure. It consists of three superimposed boundary layers: a sublayer, an 'overlap' layer and a 'wake layer'. The final function is the sum of these three parts – essentially this may be seen as an extension of Coles (1956) original law-of-the-wall, law-of-the-wake concept.

The first thing to note is that, since the three layers are added together, they must all be consistent with the boundary conditions and the conditions at the edge of the layer. Note that we will first develop the concept for turbulent boundary layers, then extend it to other wall-bounded flows (pipe and channel flows).

2.1. *The sublayer*

The form of the sublayer function is inspired by the form presented by Reichardt (1951). Reichardt constructed a function with the correct first-order Taylor series expansion (for zero-pressure-gradient boundary layers) that reached a constant value at some distance from the wall and was defined by a single parameter that could be identified with the sublayer thickness. This was then combined with the logarithmic law so that the composite profile asymptotes to a logarithmic region far from the wall.

Taylor series expansion of the boundary layer equations gives us the correct asymptotic form for the boundary layer near the wall as

$$U^+ = y^+ + \tfrac{1}{2}p_x^+ y^{+2} + a_1 y^{+4} + \text{h.o.t.}, \tag{2.5}$$

where $p_x^+ = (\nu/\rho U_\tau^3)(\mathrm{d}p/\mathrm{d}x)$ and a_1 is a coefficient assumed to be universal for zero-pressure-gradient flows.

It is surprising that none of the existing formulations take this expansion into account fully: they ignore the second term on the right as small. One reason is, perhaps, that it is only in strong pressure gradients that the p_x^+ term is significant and noticeable. In moderate- to high-Reynolds-number flows p_x^+ is generally small which has sometimes led to the mistaken conclusion that the pressure gradient does not directly affect the inner layer. Whilst this is a small effect it seems sensible to include it in the functional form when analysing flows with strong pressure gradients.

At the edge of the boundary layer we would expect the gradient $\partial U/\partial y$ to tend to zero at large y and hence the sublayer function must have an asymptotically zero gradient in this limit. The functional form chosen for the sublayer region is

$$U^+ = y_c^+\big(1-\big(1+2(y^+/y_c^+)+\tfrac{1}{2}(3-p_x^+ y_c^+)(y^+/y_c^+)^2-\tfrac{3}{2}p_x^+ y_c^+(y^+/y_c^+)^3\big)\mathrm{e}^{-3y^+/y_c^+}\big). \tag{2.6}$$

This function asymptotes to a constant value at large y^+ and has the Taylor-series expansion

$$U^+ = y^+ + \tfrac{1}{2}p_x^+ y^{+2} - \tfrac{9}{4}\big(\tfrac{1}{2}y_c^+ + p_x^+ y_c^{+2}\big)y^{+4}/y_c^{+4} + \text{h.o.t.} \tag{2.7}$$

It should also be noted that this profile is defined by one free parameter, y_c^+, which may be considered as a measure of the sublayer thickness. This is a constant for a given boundary layer profile, i.e. each profile has a unique value of y_c. It will already be apparent that changes in this sublayer thickness will lead to a shift in the log-law intercept. The sublayer defined in this way is a boundary layer in its own right since it satisfies the correct asymptotic and boundary conditions.

2.2. *The 'overlap' region*

This is the part of the boundary layer in which both the viscosity and the outer flow scales are negligible. It is often derived by an overlap argument with an outer-velocity defect law (Millikan 1938). It may, alternatively, be derived by defining a region in the flow where the 'mean relative motions' depend only the distance from the wall and one relevant constant velocity scale, generally taken as the wall-shear velocity (Townsend 1956).

This layer must then satisfy appropriate boundary and asymptotic conditions. Since the function is to be added to the sublayer function, it is important that it should not interfere with the correct boundary conditions at the wall: this places a limit on the lowest order of its Taylor-series expansion. It must also asymptote to a constant value at large y. This is an important feature that is neglected in many existing functions. Many assume a logarithmic region that extends to infinity, then add a wake function to

this. The folly in this approach becomes apparent when dealing with boundary layers in strong favourable pressure gradients. In these flows the wake can be extremely small or even non-existent. If we remove the wake then the behaviour at the edge of the layer is unphysical since the function continues to increase without bound. It makes good physical sense for the overlap layer to become asymptotically constant at the edge of the layer since the turbulent eddies which maintain the gradient (in some fashion) disappear beyond the edge of the layer. Various authors have noted this and tried to fix the behaviour but the correction has generally been in terms of a 'patch-up' solution which adds a term to make the gradient zero at the 'edge' of the layer (which it is not for boundary layers, though it may be small). These solutions to the problem (see e.g. Lewcowitz 1982) also behave anomalously beyond the edge of the layer so that arguments or analysis must avoid the limit as $y \to \infty$. This may be a minor restriction but it is still incorrect behaviour from a physical point of view. The 'logarithmic' layer should be a function that becomes asymptotically logarithmic at infinite Reynolds number. The leading-order behaviour should be greater than or equal to y^4 so that it does not disturb the correct expansion near the wall. The function chosen is

$$U^+ = \frac{1}{6\kappa} \ln \left(\frac{1 + (0.6(y^+/y_c^+))^6}{1 + \eta^6} \right). \tag{2.8}$$

This has the desired behaviour since while $y^+ \gg 1$ and $\eta \ll 1$ the function has a logarithmic form. Naturally a significant logarithmic region can only occur if the Reynolds number, δ^+, is sufficiently large. The factor 0.6 in the function is merely a small correction that makes the function fit the data slightly better. It could have been omitted for 'neatness' but since the objective is to provide an excellent fit to the data, it has been retained. The other attractive feature of this function is that it naturally splits into the form $f(y^+) + g(\eta)$ and since the wake function is a function of η then the whole profile naturally splits into this two-part form which fits neatly with classical theory.

2.3. *The wake function*

The wake function presented here is simply a good fit to the data. The only constraints on its construction are that it must have an expansion at $y = 0$ of higher than third order and it must asymptote to a constant value at large y (and do so rapidly). The form chosen is

$$w(\eta) = b \left(1 - \exp \left(-\frac{5(\eta^4 + \eta^8)}{1 + 5\eta^3} \right) \right), \tag{2.9}$$

where b is a measure of the wake strength and is equivalent to Coles' wake parameter. In this study b is found for each profile by curve-fitting the full functional form to the data. It should be noted that boundary layer profiles asymptote to the free-stream velocity very quickly which explains the role of the term η^8. This rapid approach is one reason why some researchers have chosen to set the gradient at the edge of the layer to zero even though this is not the correct asymptotic behaviour for boundary layers.

3. Pipe and channel flows

In the case of pipe and channel flows it should be expected that the overall functional form of the profile is very similar since the physical and dimensional arguments translate. The difference is that, in these flows, the correct outer condition

is that $\partial U/\partial y = 0$ at $y = R$, $y = h$, where R and h are the pipe radius and the channel half-width respectively. It turns out not to be difficult to modify the above form to take this into account, at least approximately. The sublayer function is allowed to remain the same since, even at very low Reynolds number, the contribution of this term to the gradient at the edge is negligible. The logarithmic function is modified to

$$U^+ = \frac{1}{6\kappa} \ln\left(\frac{1 + (0.6(y^+/y_c^+))^6}{1 + \eta^6 + \eta^{12}}\right) \tag{3.1}$$

which ensures a gradient very close to zero at the centreline (note here $\eta = y/R$, y/h for pipe and channel flows respectively). The actual gradient at the centreline depends on the Reynolds number and the ratio R^+/y_c^+ (or h^+/y_c^+ in channel flow). Even for very low Reynolds numbers the gradient is extremely small (for $R^+ = 100$, $\partial U^+/\partial y^+ < 10^{-6}$) and is certainly precise enough for the purpose of analysing the data. The wake function is also modified by the addition of an extra term

$$w(\eta) = b\left(1 - \exp\left(-\frac{5(\eta^4 + \eta^8)}{1 + 5\eta^3 + 10.5\eta^8}\right)\right) \tag{3.2}$$

which ensures that this term has zero gradient at the centreline. Examination of available data shows that this form is an excellent fit. The approach also makes some physical sense since it suggests that, while we are far from both the centreline and the wall, the flow is unaware of the difference between a channel (or pipe) flow and a boundary layer flow. There is, perhaps, some argument that a pipe flow should be different from a channel flow near the centreline but this function fits all the data extremely well which suggests that the differences are small. Note that Wosnik, Castillo & George (2000) suggest that the functional forms of the mean velocity profiles of pipe and channel flows are very different to those of boundary layer flows, with the former overlap region described by a log-law whereas the latter are described by a power-law. The author disagrees on this point.

4. Some comments on the final form

At this point it is worth noting how the new form fits in with the classical approach.

4.1. *High Reynolds number*

The form of the 'logarithmic' or 'overlap' region at very high Reynolds number is easy to derive. We take the approach of assuming we are in a region where $y^+ \to \infty$ and $\eta \to 0$ simultaneously. This can occur if $\delta^+ \to \infty$. In a boundary layer with a finite applied pressure gradient the p_x^+ term becomes zero since, if we define an outer pressure-gradient parameter as $\beta = (\delta^*/\rho U_\tau^2)(\mathrm{d}p/\mathrm{d}x)$ (following Clauser 1956), then $p_x^+ = \beta/\delta^{*+}$. In this case the sublayer function reduces to a constant value y_c^+ which is assumed to be a universal constant in the absence of external effects. The contribution of the 'wake function' becomes zero in this region and so the whole profile becomes

$$U^+ = \frac{1}{\kappa}\ln(y^+) + y_c^+ - \frac{1}{\kappa}\ln(y_c^+/0.6) \tag{4.1}$$

which is equivalent to the traditional form of the log-law and the value of the intercept is given in terms of y_c^+. It will be shown later that the zero-pressure-gradient data suggest that the appropriate value of y_c^+ is 12 and $\kappa = 0.39$ which gives a value of 4.32 for the intercept. These values are close to those suggested recently by Österlund *et al.* (2000) ($\kappa = 0.38$, intercept $= 4.1$) from their analysis of high-Reynolds-number

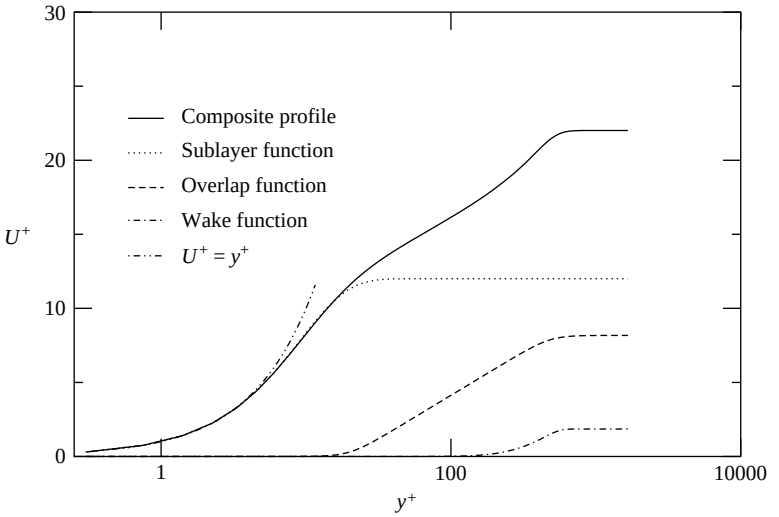

FIGURE 1. The three parts of the functional form shown with the composite profile which is the sum of all three. The composite profile is the fit to the zero-pressure-gradient data of Spalart (1988), $R_\theta = 1410$

boundary layer data. The functions and their contributions to a zero-pressure-gradient profile are shown in figure 1.

4.2. *Defect law*

The defect law may be written as $U_1^+ - U^+$, where U_1 is the external velocity, outside the boundary layer. Strictly speaking U_1^+ is the limit of U^+ as $y \to \infty$. It is not possible to use this limit with most of the common formulations since they assume a log-law extending to infinity. The new formulation has no such difficulty and it is easy to show that for large Reynolds number (it does not need to be particularly large) and away from the sublayer,

$$\frac{U_1 - U}{U_\tau} = \frac{1}{6\kappa} \ln\left(\frac{1+\eta^6}{\eta^6}\right) + b \exp\left(-\frac{5(\eta^4+\eta^8)}{1+5\eta^3}\right). \tag{4.2}$$

Note that this form is still appropriate for flows such as sink-flow boundary layers where the wake may be negligible, since the function naturally becomes zero at large η regardless of the value of b. Finally we consider the case where $\eta \to 0$ but we are still beyond the sublayer (so y^+ is large) and find the classical defect law

$$\frac{U_1 - U}{U_\tau} = -\frac{1}{\kappa} \ln(\eta) + C_1, \tag{4.3}$$

where C_1 is a constant. A similar procedure leads to the defect law for a pipe or channel flow

$$\frac{U_1 - U}{U_\tau} = \frac{1}{6\kappa} \ln\left(\frac{1+\eta^6+\eta^{12}}{3\eta^6}\right) + b\left(-0.074 + \exp\left(-\frac{5(\eta^4+\eta^8)}{1+5\eta^3+3.5\eta^{12}}\right)\right) \tag{4.4}$$

and again taking the limit as $\eta \to 0$ we have

$$\frac{U_1 - U}{U_\tau} = -\frac{1}{\kappa} \ln(1.2\eta) + 0.926b, \tag{4.5}$$

which is of course equivalent to the usual form derived from the overlap arguments leading to the logarithmic law.

4.3. *Reynolds-number dependence*

It is interesting to note that, if we ignore the effect of a pressure gradient, the form given above for the 'overlap' region may be written as

$$y^+\frac{\partial U^+}{\partial y^+} = \frac{1}{\kappa}\frac{(a^6\delta^{+6}-1)y^{+6}}{(1+a^6y^{+6})(\delta^{+6}+y^{+6})} \tag{4.6}$$

where $a = 0.6/y_c^+$ is a universal constant in the absence of pressure-gradient effects. This is of the form

$$y^+\frac{\partial U^+}{\partial y^+} = \phi(y^+, Re) \tag{4.7}$$

since δ^+ is an appropriate local Reynolds number of the boundary layer. It is not difficult to show that $\phi(y^+, Re) = 1/\kappa$ in the limit as $Re \to \infty$. This, (4.7), is the form suggested by Barenblatt (1996) as a starting point for his analysis which leads to a power-law form for the mean velocity profile in general and a log-law in the infinite Reynolds number limit. This is an important point since it has been noted by various researchers that the 'overlap' should be Reynolds-number dependent. This has led to various alternative forms for this region (other than logarithmic). Here a simple construction both illustrates and makes explicit the Reynolds-number dependence of this region and still retains the asymptotic form of a log-law. The classical law-of-the-wall law-of-the-wake formulation also contains an implicit Reynolds number dependence (since it is of the form $f(y^+) + g(\eta)$) but this disappears when the wake parameter is identically zero (as it may be in the case of sink-flow boundary layers).

5. Fitting the data

The final function then has only three potentially free parameters if it is assumed that κ is a universal constant (a point that will be returned to later). They are the sublayer parameter, y_c^+, the wake parameter, b, and, in the case of boundary layers the boundary layer thickness, δ. Hence this new functional form has the same number of degrees of freedom as the classical form. It may be expected (and will be shown) that the sublayer parameter is a function of the streamwise pressure gradient, p_x^+. At high Reynolds numbers the value of p_x^+ tends to be very small and hence the sublayer parameter will be a universal constant (which essentially plays the same role as the intercept in the traditional basic form of the log-law expression).

In order to examine the variation of parameters from data it is necessary to fit this expression to the data. The approach used here is a nonlinear curve-fitting routine which will find the best fit of any function to a data-set. The program uses the Levenburg–Marquardt algorithm based on LMDIF from MINPACK, with some modifications. All fits to the data were carefully inspected and proved to be excellent optimizations of the function.

As a starting point, data for the smooth-wall zero-pressure-gradient boundary layer were examined in order to find the appropriate value of the von Kármán constant, κ, and the appropriate value of the sublayer parameter, y_c^+. It was reasoned that there should be no additional parameters that may affect these 'universal' constants. It is worth noting at this point that we have not eliminated the possibility that κ may depend on the pressure gradient. The fitting is done allowing b and δ to vary.

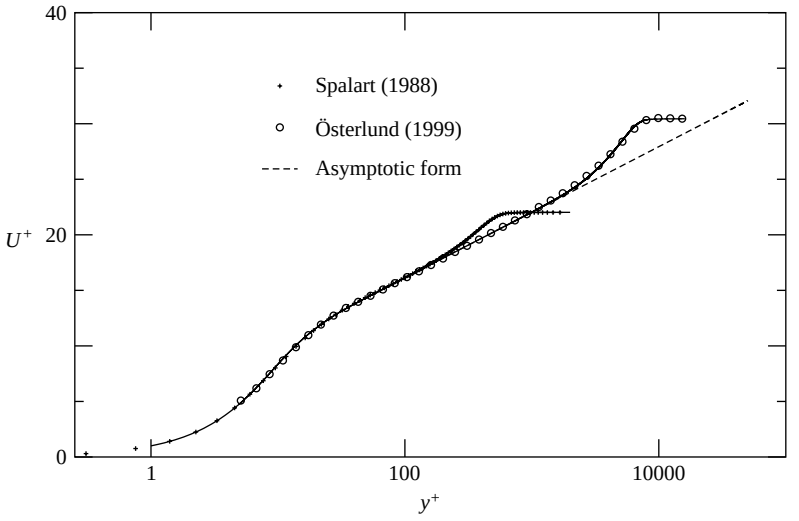

FIGURE 2. Fit of the functional form to the zero-pressure-gradient data of Spalart (1988), $R_\theta = 1410$, and Österlund (1999).

The fit of the function to the zero-pressure-gradient DNS of Spalart (1988) and the zero-pressure-gradient measurements of Österlund (1999) is shown in figure 2. This is shown simply to demonstrate the goodness of fit for typical boundary layer profiles without the pressure-gradient effects to be discussed later. Also shown is the asymptotic 'infinite'-Reynolds-number log-law using the constants selected for the model ($y_c^+ = 12$ and $\kappa = 0.39$).

5.0.1. *The data*

A wide range of data has been used in establishing the values of parameters and their variation. Much of this has been DNS data since it has two obvious advantages. The first is that the wall shear stress is known accurately for these flows so there is minimal uncertainty associated with the values of the parameters. The second is the availability of very near-wall data without the complicating effects of probe corrections etc. Also relevant is the fact that when examining pressure-gradient effects the pressure-gradient parameter, p_x^+, is generally larger at low Reynolds number, hence pressure-gradient effects are likely to be larger in low-Reynolds-number flows. This means that the restriction of DNS data to low Reynolds number is not a disadvantage. Experimental data have also been used where possible and have been selected on the basis of the minimum uncertainty in wall shear stress and general accuracy of the results. Some researchers have used a fit of the log-law (with particular values of the universal constants) to calculate the wall shear stress, which is obviously unacceptable when we are examining parametric effects in this region. A large amount of data has been used to develop the model that follows.

6. The effect of pressure gradient on the inner flow

A wide range of flows was examined in order to determine the effect of strong pressure gradients on the inner flow. Of particular interest is the change of the sublayer thickness y_c^+. It is quite well known that strong pressure gradients lead to a departure of the flow from the universal law of the wall with favourable pressure gradients

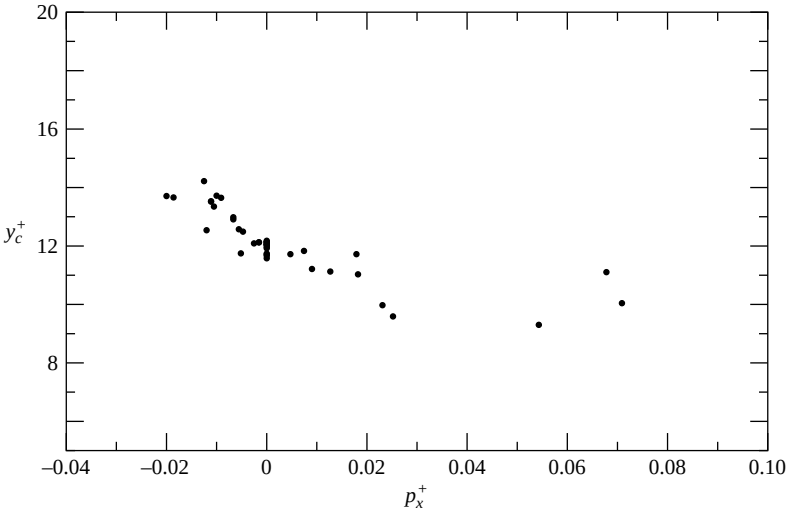

FIGURE 3. The variation of y_c^+ with p_x^+ for fixed κ.

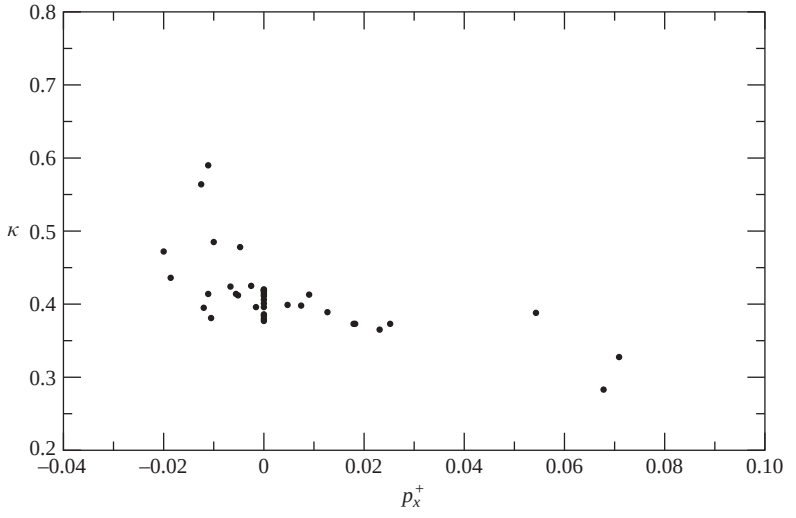

FIGURE 4. The variation of κ with p_x^+ (both κ and y_c^+ allowed to vary).

causing the mean velocity profile to fall above the standard 'log-law' and adverse-pressure-gradient flows below. The data shown in figure 3 illustrate this behaviour. The data for this figure have been derived by fitting the appropriate profiles with a fixed value of $\kappa = 0.39$ and allowing the wake parameter and the sublayer parameter to vary. The data on this plot include adverse-, favourable- and zero-pressure-gradient boundary layers, pipe flows and channel flows. Whilst there is some scatter, a clear trend is obvious overall. The zero-pressure-gradient results ($p_x^+ = 0$) give some idea of the scatter in the value of this parameter even in flows where external effects should be small.

Since there is no *a-priori* reason to assume that the value of κ should be unaffected by the pressure gradient, figure 4 shows the results when κ is also allowed to vary

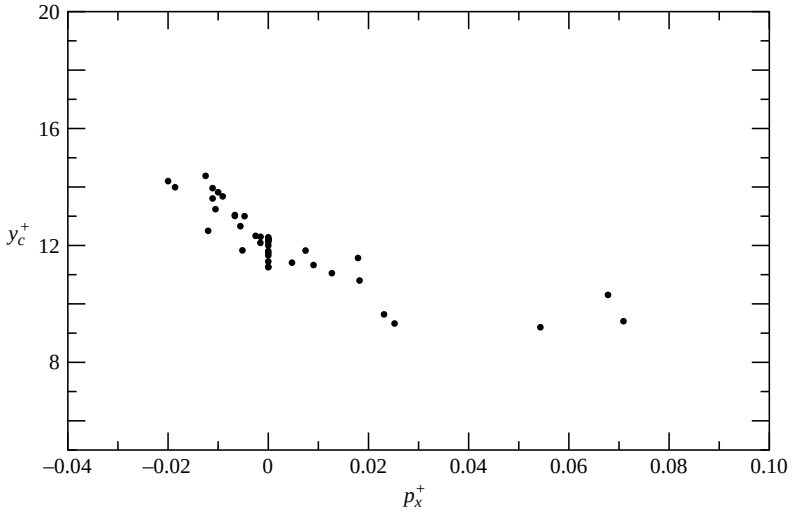

FIGURE 5. The variation of y_c^+ with p_x^+ with varying κ.

in the fitting process. The results for y_c^+ from this procedure are shown in figure 5. The data shown on these plots are the same as that shown in the later figures where the sources are identified. These figures simply show that there is a consistent overall trend with pressure gradient.

The variation is no surprise but the questions to be asked are: 'why should the sublayer thickness vary with pressure gradient'; and 'should κ also vary, and if so, why?' This brings us to the next and, perhaps, most interesting part of the paper.

7. A simple model for the change of the inner flow with pressure gradient

The model that follows was inspired by a simple, seemingly casual, observation in Clauser (1956). He pointed out that the thickness of the sublayer in zero-pressure-gradient flow is consistent with the idea that the sublayer grows until it reaches a critical Reynolds number which is approximately the minimum critical Reynolds number of a laminar boundary layer. This is an appealing idea since it links the sublayer to the laminar boundary layer. The idea is that at a certain distance from the wall the sublayer reaches a local Reynolds number at which it becomes unstable and at this point perturbations grow and turbulence is generated. It is interesting to note that the maximum production does indeed occur at a position which may be considered to be the edge of the sublayer. In fact it occurs in the range $10.5 < y^+ < 12$ (from the DNS of Spalart 1988) which coincides quite well with the value of $y_c^+ = 12$ found above for zero-pressure gradient boundary layers (it is quite interesting that a simple rough analysis by Clauser in his paper also suggested a value of 12 which was found here by different means).

This idea immediately gives an inkling of an explanation for the change in y_c^+ with pressure gradient. The addition of an adverse pressure gradient to a laminar boundary layer reduces the critical Reynolds number for instability and a favourable pressure gradient increases it. Hence it seems plausible that in an adverse pressure gradient the sublayer would reach its critical Reynolds number sooner, i.e. closer to the wall, and in a favourable pressure gradient it would occur later, i.e. further from the wall.

Two things are immediately obvious. The first is that the sublayer is not exactly a laminar boundary layer – though it is something like one since it is a wall-bounded region dominated by viscosity. Secondly it is not a trivial matter to apply a stability analysis to the sublayer since it is has difficult-to-define boundary conditions and is subjected to vigorous stirring from the outer flow (it is unlikely to be possible at all using the usual approaches to laminar boundary layer stability analysis). So the idea has some appeal in a physical sense but it is difficult to make any quantitative use of the concept.

The next essential idea comes from a paper by Van Driest & Blumer (1963). In this paper the authors develop a way of predicting the effect of both pressure gradient and turbulence intensity on the transition of laminar boundary layers. The approach is quite clever and involves defining a new Reynolds number for the boundary layer in terms of the vorticity of the layer and the distance from the wall. In this way a single critical Reynolds number for the boundary layer can be defined and the effect of the pressure gradient is to modify the profile such that the critical Reynolds number occurs closer to the wall in an adverse pressure gradient or further from the wall in a favourable pressure gradient. This simple approach gives reasonable agreement with the calculations from linear stability theory and allows the inclusion of effects such as free-stream turbulence.

It turns out that this Reynolds number can also be expressed in terms of the local total shear stress (or the local total shear-stress velocity) which is more useful when examining the sublayer of a turbulent boundary layer. In the case of a zero-pressure-gradient boundary layer this would be equal to the wall shear stress (to a close approximation) and hence a local Reynolds number would simply be y^+. Thus we would expect the sublayer 'edge' to occur at a critical fixed value of y^+ which would appear to be around 11 to 12 from the data. This critical value of y^+ is denoted by y_c^+ as was used earlier in the functional form. Qualitatively, then, we know that the local total shear stress is increased in an adverse pressure gradient and hence expect the sublayer to reach the critical value closer to the wall at a smaller value of y^+ and vice versa for a favourable pressure gradient.

Having, hopefully, established the physical reasoning and the origin of these ideas the next step is to express the model mathematically so concrete predictions can be made. Since we wish to look at the local value of the total shear stress near the wall we can use the expansion of the local total shear stress which is

$$\frac{\tau}{\tau_w} = \frac{\nu \partial U/\partial y - \overline{uv}}{U_\tau^2} = 1 + p_x^+ y^+ + \text{h.o.t.} \tag{7.1}$$

This equation is derived directly from the momentum equation. Note that it is the total shear stress that is important, not just the viscous contribution from the mean velocity gradient. The appropriate critical Reynolds number can then be defined as

$$R_c = \frac{U_T y_c}{\nu} \tag{7.2}$$

where $U_T = \sqrt{\tau(y = y_c)/\rho}$ and y_c is the critical value of y at which the sublayer becomes unstable. R_c is assumed to have a universal value for all wall-bounded flows. The value is easily obtained from the zero-pressure-gradient data since, in this case, $U_T = U_\tau$ and hence $R_c = y_c^+(\text{ZPG}) = 12$. The value 12 is chosen since it is around the middle of the small scatter for zero-pressure-gradient data and is also a round number. The value can be refined slightly but for the purpose of explaining the model and achieving some quantitative predictions this value will suffice.

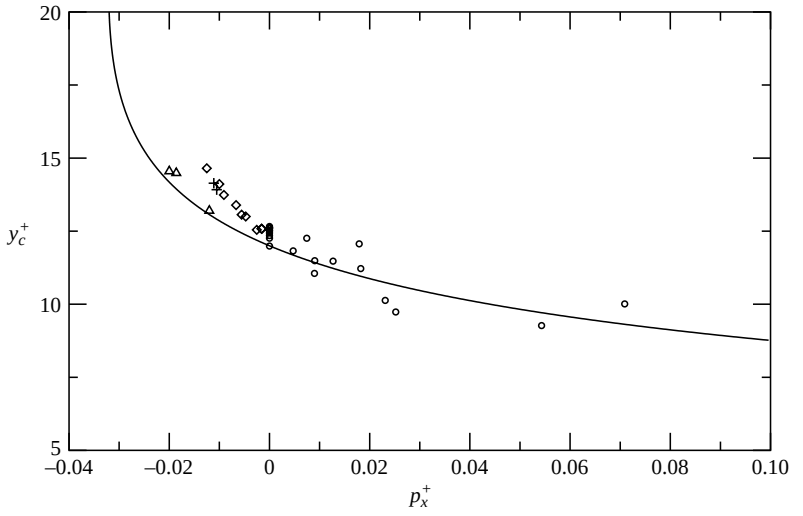

FIGURE 6. The variation of y_c^+ with p_x^+ as given by the model (solid line) compared with the data. △, Sink-flow boundary layers (Spalart 1986); +, pipe flows (Eggels *et al.* 1994 and Loulou *et al.* 1997); ⋄, Channel flows from the Database of Turbulence and Heat Transfer; ○, boundary layer flows (Skote *et al.* 1998 and Nagano *et al.* 1991).

Now if we substitute the expression for the local stress we arrive at the equation

$$R_c = \frac{U_T y_c}{\nu} = \frac{y_c U_\tau}{\nu}\sqrt{1 + p_x^+ y_c^+ \ldots} \tag{7.3}$$

and hence we have an equation for y_c^+. This is more conveniently written in the form

$$p_x^+ y_c^{+3} + y_c^{+2} - R_c^2 = 0. \tag{7.4}$$

Since this is a cubic equation there are obviously three possible solutions. At present we will assume that the appropriate solution is the smallest positive solution for a given p_x^+ and R_c. This seems reasonable given that this is the value that will be reached first as the sublayer grows. Figure 6 shows the locus of the solution of this equation for the value of $R_c = 12$. Note that R_c is the only free parameter and since this is obtained from the zero-pressure-gradient case there is very little freedom to adjust the function to better fit the data. The correlation with the data is quite reasonable given the simplicity and inflexibility of the model. In fact the prediction is as good as any of the available empirical correlations known to the author. There is some scatter in the results, particularly for strong adverse pressure gradients. The worst agreement is for strongly non-equilibrium flows. Equilibrium here is used in the traditional sense that the mean velocity profile in defect form collapses as do the Reynolds stresses. Also all appropriate non-dimensional parameters remain constant with streamwise distance. Strongly non-equilibrium flows are ones in which the external parameters change quickly and the non-dimensional parameters characterizing the flows do not remain constant. It is not surprising that such a simple model does not predict such flows accurately since it is based on the idea that the local sublayer thickness depends only on the local pressure-gradient parameter. In flows where the parameters are changing quickly then non-local and historical effects must play a role in the development. The worst case gives an error of around 9% in the value of y_c^+ as predicted by the model

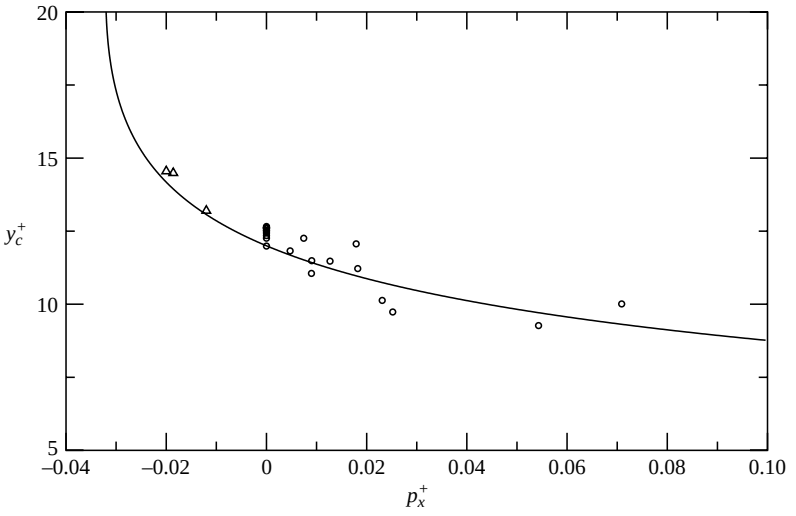

FIGURE 7. The variation of y_c^+ with p_x^+ as given by the model compared with the data for boundary layer flows only.

when compared with the value from fitting the experimental profiles. Note that this plot shows data from boundary layers, pipe flows and channel flows.

The channel and pipe flow data fall consistently above the predicted variation. If we exclude these flows and show only boundary layer profiles the collapse on the prediction is even better as shown in figure 7. It is possible that channel and pipe flows may have a slightly higher value of R_c than boundary layers. A value of $R_c = 12.8$ improves the agreement for these flows substantially but it is not known at this stage if a different value is appropriate.

7.1. *Variation of* κ

Initially, the idea that the von Kármán constant, κ, is also affected by a pressure gradient was resisted by the author. It was thought that there are too many functional forms that allow an arbitrary variation in this parameter that may be adjusted to fit any particular model. Consideration of the physical model, however, suggests that there should be an effect of the pressure gradient on this parameter. The argument is that, if the model defines a length scale for the inner flow as y_c, the sublayer thickness, then it also defines a velocity scale for the inner flow as U_T. We must now be more explicit about the description of the physical model. The idea is this: the viscous sublayer grows to a point where it reaches the critical Reynolds number based on the value of the total stress and the distance from the wall. At this point the flow is unstable to perturbations and the instability generates some form of turbulent eddies which grow out from this point to form the turbulent flow outside of the sublayer. These eddies grow in such a way that their length scale grows with their distance from the wall and hence they are 'attached eddies' in the sense of Townsend (1976). The velocity scale of these eddies is determined by the critical velocity scale of the sublayer and so we end up with an array of eddies of different sizes but with the same velocity scale, i.e. U_T. This model then leads naturally to a log-law since the mean velocity gradient in the region can only be specified by the velocity scale and the distance from the wall, i.e. $\partial U/\partial y = U_T/\kappa_o y$. Note the subscript '$o$' has been used to denote that this is a universal constant unaffected by pressure gradient (or Reynolds number). The

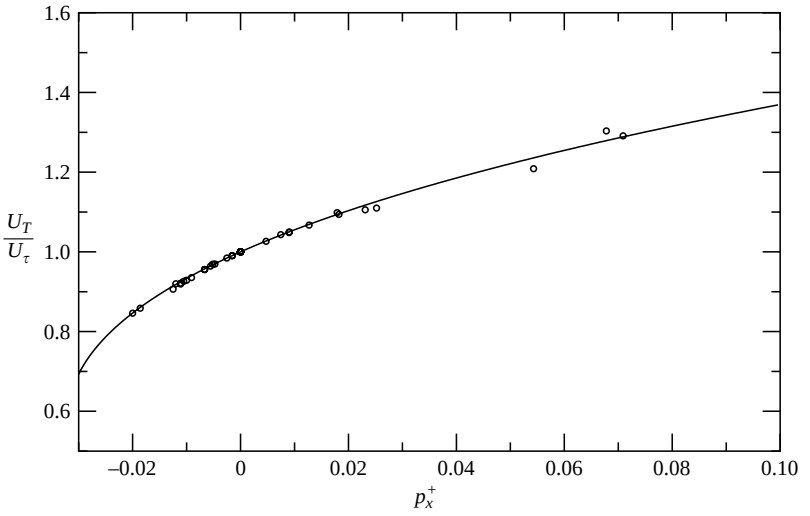

FIGURE 8. The variation of U_T/U_τ with p_x^+ from the data compared with the model (solid line).

actual κ that appears in the traditional formulation is defined by $\partial U/\partial y = U_\tau/\kappa y$ and comparing these two formulations suggests that $\kappa/\kappa_o = U_\tau/U_T$. The universal value can be found from zero-pressure-gradient data which suggests a value of around 0.39. There is still some dispute about the appropriate value but this will suffice for the present. It appears to fit the data very well. What the model then suggests is that strong adverse-pressure-gradient flows should have an appropriate value of κ which is somewhat less than 0.39 and strong favourable pressure gradients a value which is somewhat more than 0.39. In fact in terms of the parameters of the model the relationship is

$$\frac{\kappa}{\kappa_o} = \sqrt{\frac{1}{1 + p_x^+ y_c^+}}. \tag{7.5}$$

This is no arbitrary variation that may be adjusted to suit the model. Since y_c^+ is fully defined by (7.4) then, once we have chosen the value of κ_o from the best available zero-pressure-gradient data, the variation of κ is completely defined. Again it is worth emphasizing the strongly constrained nature of the model. There are at best only two 'free' parameters R_c and κ_o but these are obtained from zero-pressure-gradient data and can only be chosen within the natural scatter of the measurements (this gives about a $\pm 6\%$ variation for R_c and a $\pm 3\%$ variation in κ_o). The values of y_c^+ versus p_x^+ shown in figures 6 and 7 were obtained by fitting the profile with the value of κ as given by (7.5). Figure 8 shows the variation of the velocity scale, U_T, as found by fitting the data compared with the prediction of the model. The data shown are the same as those used in figure 6, which include pipe and channel flows. The agreement is excellent, but this quantity is much less sensitive to errors in the prediction than y_c^+. Values from this plot are used later to non-dimensionalize the Reynolds stresses.

8. The fit of the new form to the mean flow data

The equation for the sublayer parameter and the von-Kármán constant allow us to fit the whole boundary layer profile given a value of p_x^+. The parameters allowed

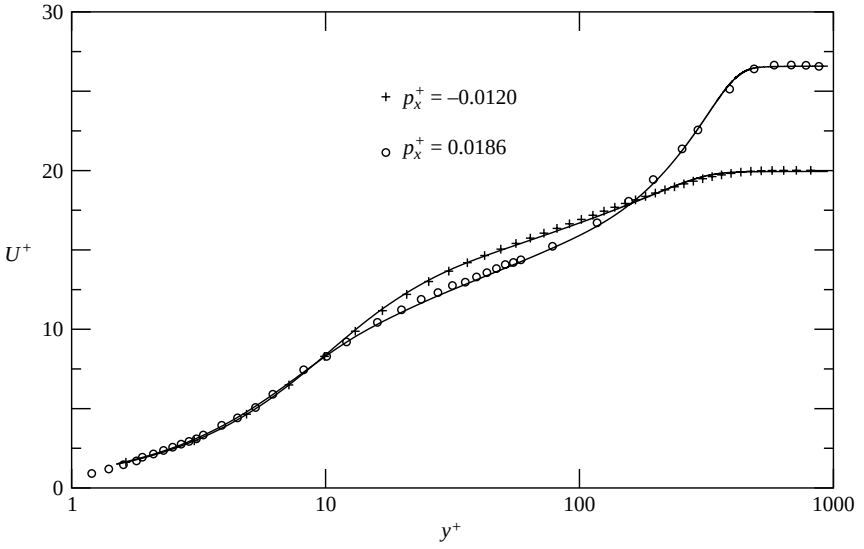

FIGURE 9. The fit of the function to favourable- (Spalart 1986) and adverse-pressure-gradient (Nagano *et al.* 1991) boundary layer profiles.

to vary in the fitting procedure are the wake parameter and the boundary layer thickness (actually δ^+ which is equivalent). Allowing the boundary layer thickness as a parameter in the model may strike some readers as cheating. It may be argued that the boundary layer thickness should be independently defined, for example as the 99.5% thickness or an integral thickness such as that defined by Clauser (1956). The difficulty with trying to define an independent thickness of this nature comes from the structure of the boundary layer itself. This is particularly evident in the present situation where the Reynolds number is low and the sublayer makes a significant contribution to the boundary layer thickness. Any overall integral length or percentage thickness will be made up from contributions from the sublayer, overlap layer and outer (wake) region. Hence a length of this nature is not a real measure of the outer flow length-scale alone. Fitting the functional form to the boundary layer in order to extract an outer length scale is a more sensible approach since the function explicitly defines a sensible outer length scale. At high Reynolds number the contribution of the sublayer is much smaller and so 'independently' defined thicknesses may be used. In all cases examined here the boundary layer thickness found from the fitting procedure was within $\pm 3\%$ of the 98.5% thickness of the particular layer. In the case of pipe and channel flows this parameter was fixed at the value of the pipe radius or channel half-height. Figure 9 shows the fit to data using the functional form with the values predicted by the model. The two profiles have been chosen to have reasonably strong pressure gradients and they are ones for which the model prediction for y_c^+ is quite close. This choice is not meant to mislead the reader as to the accuracy of the approach but these profiles better illustrate the goodness of fit of the shapes of the profiles, rather than those that fall further from the predicted curve.

9. Near-wall Reynolds stresses

The above analysis predicts a length scale, y_c, and a velocity scale, U_T, which define the sublayer. It is interesting to consider the relevance of these scales for

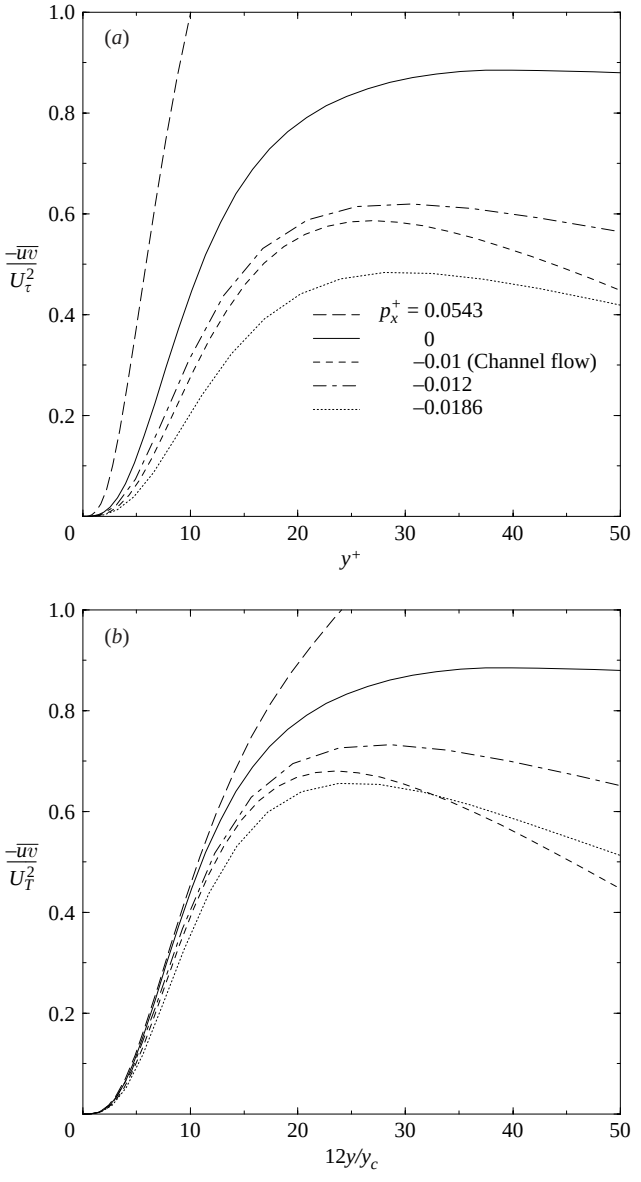

FIGURE 10. The Reynolds shear stress for strong favourable-, zero- and strong adverse-pressure-gradient flows with standard (*a*) and the new (*b*) inner-flow scaling.

the behaviour of the Reynolds stresses near the wall. It is important to note that any inner scaling should apply only very near the wall since the flow further out is influenced by the outer scales (this is particularly true of low-Reynolds-number flows since the separation between inner and outer scales is small). This effect is related to the 'inactive motions' as discussed by Townsend (1976).

In favourable-pressure-gradient flow the stresses are reduced near the wall, i.e. the initial increase in the stresses at $y = 0$ is smaller than for zero-pressure-gradient flows and for adverse-pressure-gradient flows the increase is larger. This is shown in figure 10 where the Reynolds shear stresses for strong adverse-, strong favourable- and

zero-pressure-gradient flows are shown plotted with the standard inner scaling. The five flows chosen are zero pressure gradient (Skote, Henkes & Henningson 1998), strong adverse pressure gradient (Skote *et al.* 1998), channel flow with strong favourable pressure gradient (Kuroda, Kasagi & Hirata 1990) and two favourable-pressure-gradient boundary layers (Spalart 1986). The difference is very obvious. Standard inner scaling assumes that the appropriate length scale is the viscous length scale ν/U_τ and the appropriate velocity scale is the wall-shear velocity, U_τ. The model of the flow presented here suggests that the appropriate scales should be U_T and y_c. Figure 10 also shows the Reynolds shear stresses near the wall scaled with this new scaling. The values used for y_c^+ are those found from the mean velocity profile rather than the model though the differences are small. In the new scaling the x-coordinate has been multiplied by twelve so the numbers on the axis are comparable with the values shown on the other plot using conventional inner flow scaling. The collapse is very good near the wall. A similar scaling can be applied to the RMS streamwise velocity fluctuation as shown in figure 11. Here again the new scaling brings the turbulence quantities into close correspondence near the wall.

9.1. *The other components of the turbulence*

The above simple scaling does not appear to bring the v_{rms} and w_{rms} fluctuations into such close correspondence. The effect of a pressure gradient on these components is much stronger. Since these components must be strongly affected by the presence of streamwise vortices then it is possible that the the wall-shear velocity also plays a role in their development (U_T relates to conditions at the edge of the sublayer). Hence it is reasonable to suggest that these components may also be a function of the ratio U_T/U_τ. Examining the variation of the levels of these quantities close to the wall suggests that the appropriate scaling is

$$\frac{\sqrt{\overline{v'^2}}}{U_T}\left(\frac{U_\tau}{U_T}\right)^2 = f_1(y/y_c) \tag{9.1}$$

and

$$\frac{\sqrt{\overline{w'^2}}}{U_T}\left(\frac{U_\tau}{U_T}\right)^2 = f_2(y/y_c) \tag{9.2}$$

where $f_1(y/y_c)$ and $f_2(y/y_c)$ are universal functions. Of course, as already noted, this scaling only applies near to the wall: further out the outer flow will dominate the behaviour. The collapse of the data with the above scaling is shown in figures 12 and 13. The precise reason for the difference in scaling of these components is not completely clear at this stage.

10. Towards separation

An interesting feature of the model is its behaviour as the wall shear stress goes to zero. As $U_\tau \to 0$, the velocity scale then becomes $U_T = R_c^{1/3} U_p$ and substituting into (7.4) we find

$$y_c = \frac{\nu R_c^{2/3}}{U_p}, \tag{10.1}$$

where $U_p^3 = (\nu/\rho)(\partial p/\partial x)$. Now since the whole inner profile may be expressed in terms of y/y_c we have the interesting result that in this limit the profile may be expressed completely in terms of $yU_p/\nu = y_p$. In particular a measure of the thickness

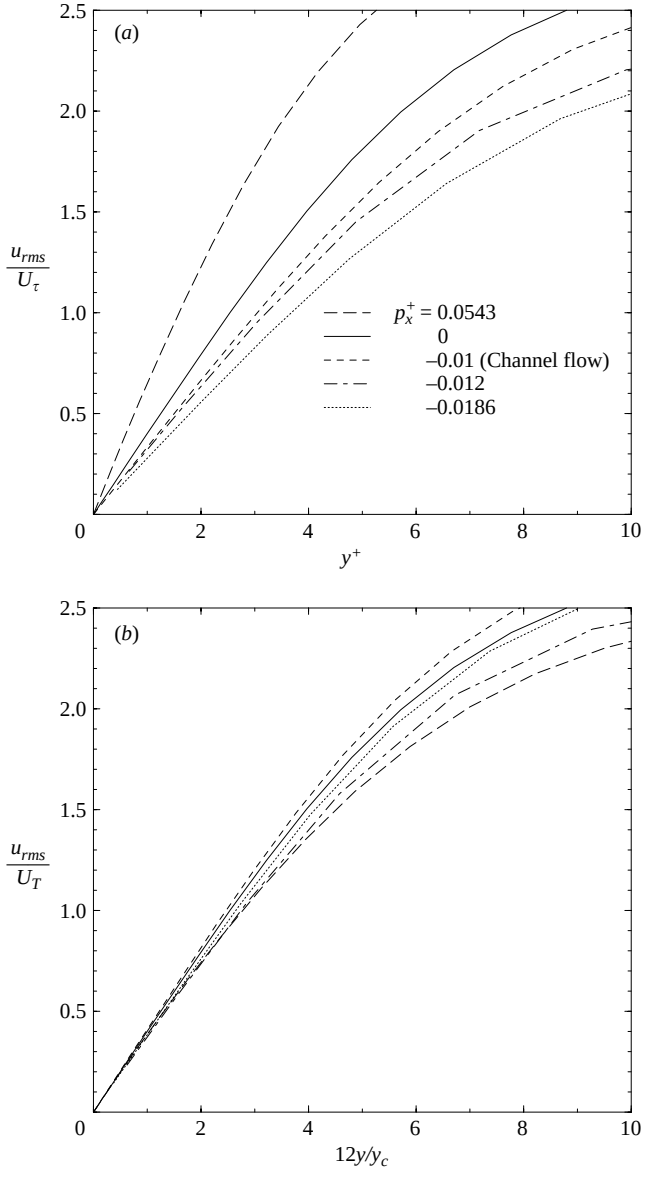

FIGURE 11. The RMS streamwise fluctuating velocity for strong favourable-, zero- and strong adverse-pressure-gradient flows with standard (*a*) and the new (*b*) inner-flow scaling.

of the 'viscous sublayer' is ν/U_p which is a sensible result since the only velocity scale in this situation should be U_p. Substitution of this into the expression for the mean velocity profile suggests that in this situation the log-law still persists but becomes a logarithmic law in yU_p/ν. In the overlap region, ($y_p \to \infty$, $\eta \to 0$), the function becomes

$$\frac{U}{U_p} = \frac{R_c^{1/3}}{\kappa_o} \ln\left(0.6 y_p / R_c^{2/3}\right). \tag{10.2}$$

The appropriate Reynolds number for this boundary layer should be $U_p\delta/\nu$ so we would only expect a logarithmic region where this parameter is large, i.e. in a

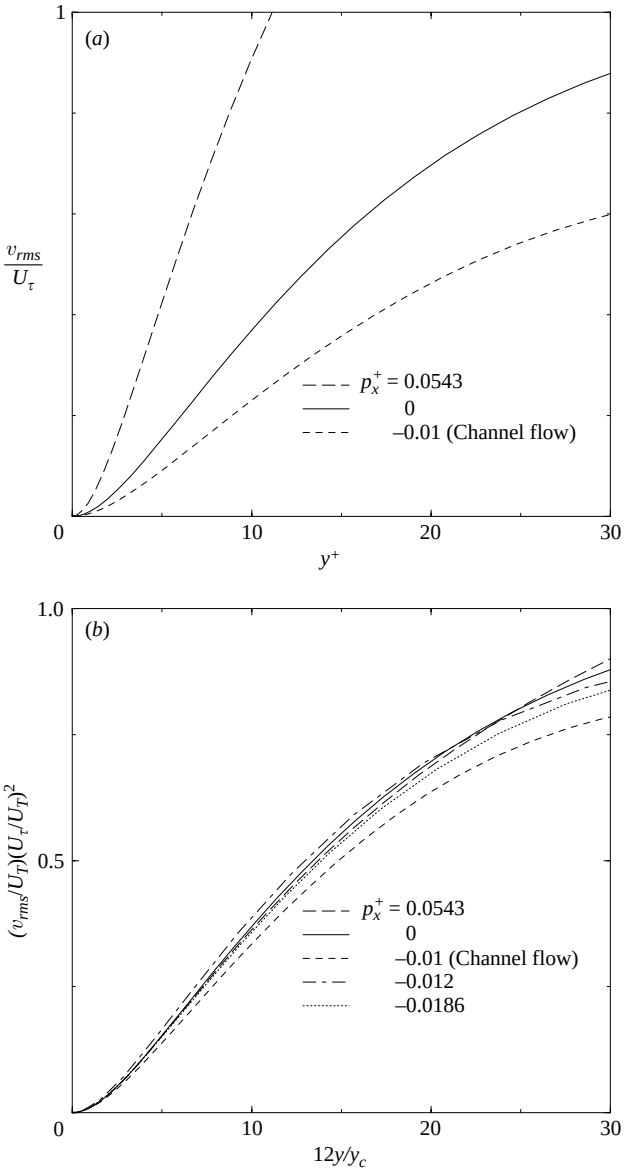

FIGURE 12. The RMS normal-to-the-wall velocity for strong favourable-, zero- and strong adverse-pressure-gradient flows with standard (*a*) and the new (*b*) inner scaling.

strong pressure gradient. It is interesting that Tennekes & Lumley (1972) showed that traditional overlap arguments lead to a similar logarithmic form for boundary layers with zero wall shear stress and strong pressure gradient. From the data of Stratford (1959) they estimated a value of 5 for the constant in front of the logarithm. This model using the value of $R_c = 12$ suggests a value of 5.87. The fact that this approach gives a sensible velocity scale and logarithmic overlap is interesting, but further work is needed to establish the correct behaviour for the sublayer function and the logarithmic intercept. This work is in progress.

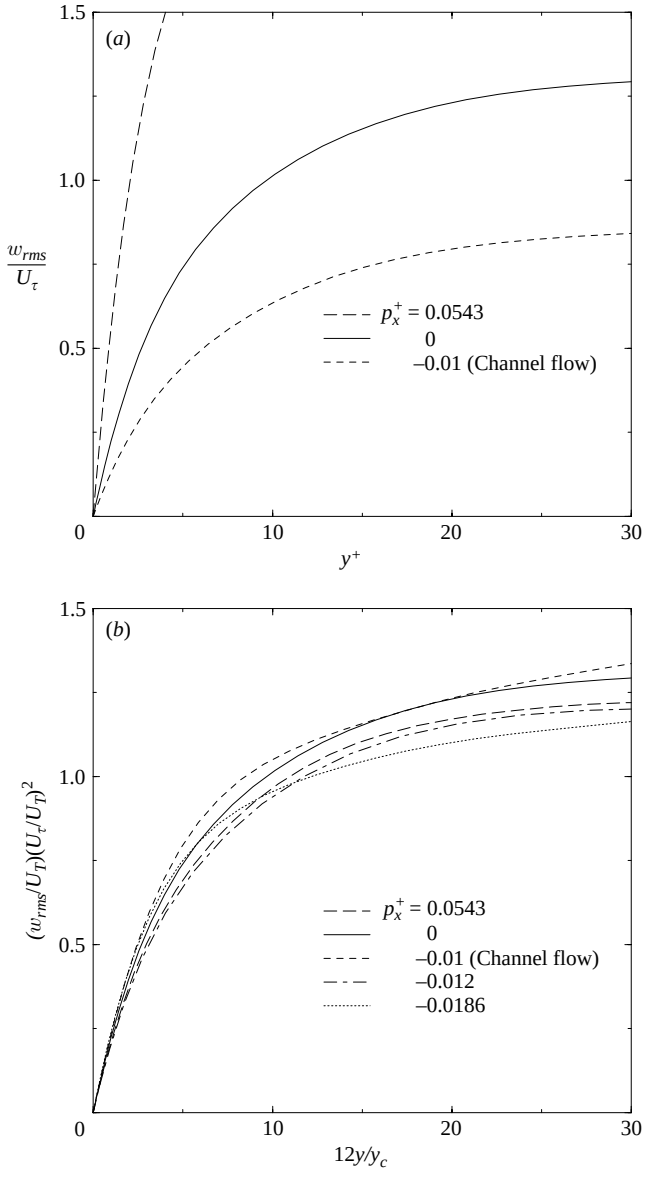

FIGURE 13. The RMS spanwise fluctuating velocity for strong favourable-, zero- and strong adverse-pressure-gradient flows with standard (*a*) and the new (*b*) sublayer scaling.

.

11. Conclusions

This paper presents a useful, sensible, self-consistent functional form for the mean-velocity profile for turbulent wall-bounded flows that allows for a consistent parameterization of data.

The results of this parameterization and the physics of the functional form have led to a new simple model to explain the effects of pressure gradients on the inner region of turbulent wall-bounded flows. The model also provides quantitative predictions of these effects which are in reasonable accord with experimental (and numerical)

results. This is particularly satisfying given that the model has only *one universal constant* (in addition to the universal von Kármán constant) which is found from zero pressure-gradient flows.

The model is defined and made completely explicit in the paper so that it may be compared to further data in order to prove or disprove the assumptions. The final functional form for the mean velocity profile may be summarized as

$$U^+ = y_c^+\left[1-\left(1+2(y^+/y_c^+)+\tfrac{1}{2}(3-p_x^+y_c^+)(y^+/y_c^+)^2-\tfrac{3}{2}p_x^+y_c^+(y^+/y_c^+)^3\right)\mathrm{e}^{-3y^+/y_c^+}\right] + \frac{\sqrt{1+p_x^+y_c^+}}{6\kappa_o}\ln\left(\frac{1+(0.6(y^+/y_c^+))^6}{1+\eta^6}\right)+b\left(1-\mathrm{e}^{-\frac{5(\eta^4+\eta^8)}{1+5\eta^3}}\right), \quad (11.1)$$

where $\kappa_o = 0.39$ and y_c^+ may be found from equation (7.4) if the value of p_x^+ is known.

One of the most attractive features is the physical basis of the model which provides an understanding of why and how different parametric effects might modify the inner region of turbulent wall-bounded flows. The model with the proposed functional form gives a good description of wall-bounded flows in the approximate range of pressure-gradient parameter $-0.02 < p_x^+ < 0.06$.

This type of work depends on a close examination of a wide range of data. The author has had access to these data through the generosity of various researchers in making their data freely available. This generosity has been further organised through the establishment of a range of databases throughout the world that can be readily accessed via the Internet. In particular the author has made extensive use of the following databases: The ERCOFTAC database, the Data-Base of Turbulence and Heat Transfer (supported by the Ministry of Education Science and Culture in Japan) and the AGARD database of test-cases for large eddy simulation. In addition Dr Martin Skote provided me with a link to his thesis data for which I am very grateful.

REFERENCES

Barenblatt, G. I. 1996 *Scaling, Self Similarity and Intermediate Asymptotics*. Cambridge University Press.

Buschmann, M. H. & Gad-el-Hak, M. 2003 Debate concerning the mean-velocity profile of a turbulent boundary layer. *AIAA J.* **41**, 565–572.

Clauser, F. H. 1956 The turbulent boundary layer. *Adv. Appl. Mech.* **4**, 1–51.

Coles, D. E. 1956 The law of the wake in the turbulent boundary layer. *J. Fluid Mech.* **1**, 191–226.

Eggels, J., Unger, F., Weiss, M. H., Westerweel, J., Adrian, R. J., Freidrich, R. & Nieuwstadt, F. T. M. 1994 Fully developed pipe-flow: A comparison between direct numerical simulation and experiment. *J. Fluid Mech.* **268**, 175–207.

Fernholz, H. H. & Warnack, D. 1998 The effects of a favorable pressure gradient and of the Reynolds number on an incompressible axisymmetric boundary layer. Part 1. The turbulent boundary layer. *J. Fluid Mech.* **359**, 357–381.

George, W. K. & Castillo, L. 1997 Zero-pressure-gradient turbulent boundary layer. *Appl. Mech. Rev.* **50**, No. 12, pt 1, 689–729.

Huffman, G. D. & Bradshaw, P. 1972 A note on von Kármán's constant in low Reynolds number turbulent flows. *J. Fluid Mech.* **53**, 45–60.

Kuroda, A., Kasagi, K. & Hirata, M. 1990 Investigation of dynamic effects of the mean shear rate on the wall turbulence via direct numerical simulation. *Proc. 27th Natl Heat Transfer Symp. of Japan*, vol. 1, pp. 46–48.

Lewkowicz, A. K. 1982 An improved universal wake function for turbulent boundary layers and some of its consequences. *Z. Flugwiss. Weltraumforsch.* **6**, 261–266.

Loulou, P., Moser, R., Mansour, N. & Cantwell, B. 1997 Direct simulation of incompressible pipe flow using a b-spline spectral method. *NASA Tech. Rep.* TM 110436.

Millikan, C. B. 1938 A critical discussion of turbulent flows in channels and circular tubes. In *Proc. 5th Intl Congress for App. Mech.* (ed. J. P. den Hartog & H. Peters), pp. 386–392. Wiley/Chapman & Hall.

Nagano, Y., Tagawa, M. & Tsuji, T. 1991 Effects of adverse pressure gradients on mean flows and turbulence statistics in a boundary layer. *Proc. 8th Symp. on Turb. Shear Flows,* pp. 7–20. Springer.

Ohtsuka, A., Iida, O., Tsuji, T. & Nagano, Y. 1995 The mechanism of retransition in wall turbulence. *Proc. 9th Symp on Computational Fluid Dynamics*, pp. 499–500.

Österlund, J. M. 1999 Experimental studies of zero pressure-gradient turbulent boundary layer flow. PhD thesis, Department of Mechanics, Royal Institute of Technology, Stockholm.

Österlund, J. M., Johansson, A. V., Nagib, H. M. & Hites, M. H. 2000 A note on the overlap region in turbulent boundary layers. *Phys. Fluids* **12**, 1–4.

Reichardt, H. 1951 Vollstandige darstellung der turbulenten geschwindigkeitsverteilung in glatten leitungen. *Z. Angew. Math. Mech.* **31**, 208–219.

Skote, M., Henkes, R. A. W. M. & Henningson, D. S. 1998 Direct simulation of self-similar turbulent boundary layers in adverse pressure gradients. *Flow, Turbulence Combust.* **60**, 47–85.

Spalart, P. R. 1986 Numerical study of sink flow boundary layers. *J. Fluid Mech.* **172**, 307–328.

Spalart, P. R. 1988 Direct numerical study of a turbulent boundary layer up to $Re_\theta = 1410$. *J. Fluid Mech.* **187**, 61–98.

Spalart, P. R. & Watmuff, J. H. 1993 Experimental and numerical study of a turbulent boundary layers with pressure gradients. *J. Fluid Mech.* **249**, 337–371.

Stratford, B. 1959 The prediction of separation of the turbulent boundary layer. *J. Fluid Mech.* **5**, 1–16.

Tennekes, H. & Lumley, J. L. 1972 *A First Course in Turbulence*. The MIT Press.

Townsend, A. A. 1956 *The Structure of Turbulent Shear Flow*. Cambridge University Press.

Townsend, A. A. 1976 *The Structure of Turbulent Shear Flow*, 2nd Edn. Cambridge University Press.

Van Driest, E. R. 1956 On turbulent flow near a wall. *J. Aerosp. Sci* **23**, 1007–1012.

Van Driest, E. R. & Blumer, C. B. 1963 Boundary layer transition, free-stream turbulence and pressure gradient effects. *AIAA J.* **1**, 1303–1306.

Wosnik, M., Castillo, L. & George, W. 2000 A theory for turbulent pipe and channel flows. *J. Fluid Mech.* **421**, 115–145.